Value of oxygen-enhanced MRI of the lungs in patients with pulmonary hypertension – a qualitative and quantitative approach

Daniel Maxien, MD[1]*, Olaf Dietrich, PhD[2]*, Sven F. Thieme, MD[1], Stefan Förster, MD[3], Jürgen Behr, MD[4], Maximilian F. Reiser, MD[1,2], Konstantin Nikolaou, MD[1]

[1] Department of Clinical Radiology, University Hospitals Munich, Grosshadern Campus, Munich, Germany

[2] Josef Lissner Laboratory for Biomedical Imaging, Department of Clinical Radiology, University Hospitals Munich, Grosshadern Campus, Munich, Germany

[3] Department of Nuclear Medicine, University Hospitals Munich, Grosshadern Campus, Munich, Germany

[4] Department of Internal Medicine 1, University Hospitals Munich, Grosshadern Campus, Munich, Germany

* D. M. and O. D. share first authorship.

Final version*: J Magn Reson Imaging* 2012; **35**(1): 86–94, <URL:http://dx.doi.org/10.1002/jmri.22740>

Abstract:

Purpose: To assess the clinical value of oxygen-enhanced MRI (oeMRI) in patients with pulmonary hypertension (PH) by correlation with ventilation/perfusion (V/Q) scintigraphy.

Materials and Methods: 33 patients with known PH underwent V/Q scintigraphy and oeMRI. Multislice oeMRI was used to assess the regional pulmonary function based on relative-signal-enhancement (RSE) and cross-correlation-coefficient (CCC) maps, evaluating mean RSE (mRSE), fraction of oxygen-activated pixels (fOAP) and mean CCC (mCCC). A visual detection of diseased lung areas was performed by two reviewers, blinded to the results of scintigraphy.

Results: In 26 of the 33 patients (79%), image quality of oeMRI reached a diagnostic level. In total, 150 lung areas were analyzed and compared; ventilation scintigraphy showed 37 diseased and 113 healthy areas (perfusion scintigraphy: 96 diseased, 54 healthy). Sensitivities/specificities of oeMRI for detecting these defects were: RSE vs. ventilation scintigraphy 92%/73%; RSE vs. perfusion scintigraphy 60%/87%; CCC vs. ventilation scintigraphy 89%/81%; CCC vs. perfusion scintigraphy 50%/87%.

The number of diseased lung areas in oeMRI correlated significantly with the number in V/Q scintigraphy ($p<0.01$). mRSE showed a significant correlation with the number of diseased lung areas in ventilation scintigraphy ($p<0.05$).

Conclusions: oeMRI is feasible in PH patients, yielding an overall moderate agreement between oeMRI and V/Q scans, with a good sensitivity of oeMRI for the detection of ventilation defects as compared with ventilation scintigraphy.

Key words:

Oxygen-enhanced MRI, Pulmonary hypertension, Lung disease, Ventilation/perfusion scintigraphy

Corresponding author:

Daniel Maxien, MD, Department of Clinical Radiology, University Hospitals Munich, Grosshadern Campus, Marchioninistr. 15, 81377 Munich, Germany

Introduction

Pulmonary hypertension (PH) is a severe disease, defined by a progressive increase of the mean pulmonary arterial pressure (≥25 mmHg at rest) with accompanying increase of pulmonary vascular resistance over 3 WU (Wood's unit) (1, 2), which may lead to right ventricular failure and eventually death. Multiple causes of pulmonary hypertension are known, ranging from idiopathic pulmonary arterial hypertension (IPAH) to disease-associated causes as in chronic thromboembolic pulmonary hypertension (CTEPH) (1). The medical management of PH is based on the underlying condition, e.g., surgery for CTEPH or vasodilating drugs for IPAH (1-3). Thus, a valid differentiation between the various causes of PH is highly desirable. Today, this requires a series of clinical examinations and imaging procedures for an accurate diagnosis. For diagnostic purposes and surveillance of patients suffering from PH, various techniques are used, such as echocardiography, right cardiac catheterization, or spiroergometry. Additional common imaging methods are computed tomography (CT) and ventilation/perfusion scintigraphy (V/Q scintigraphy). With the exception of spiroergometry and echocardiography all of the before mentioned diagnostic techniques include limiting factors for follow-up examinations, e.g. the usage of ionizing radiation in CT and V/Q scintigraphy or the invasive nature of right cardiac catheterization. In addition, there are other important disadvantages. Spiroergometry contains no information about morphology, while V/Q scintigraphy is limited to two-dimensional projection images. The necessary usage of iodinated contrast material in CT is a further potential limitation. On the other side, magnetic resonance imaging (MRI) would be a non-invasive alternative imaging method in these patients, providing morphological and functional information of the lungs at the same time, without ionizing radiation or usage of iodinated contrast material.

However, MRI of the lung suffers from low signal intensities and severe susceptibility artifacts, caused by the heterogeneous structure of the lung, which consists mainly of microscopic air-filled alveoli with a large interface between air spaces and tissue or blood (4-14). Therefore, MRI is generally considered not ideally suited for lung imaging and it would be desirable to improve MRI techniques to utilize its advantages (no radiation and possibility of functional imaging) for pulmonary applications as well. oeMRI allows for a visualization of the primary lung function, i. e., gas exchange. The gas exchange is an interaction of three mechanisms. The inhaled oxygen must reach the alveoli (*ventilation*). The oxygen has to pass over from the alveoli into the capillaries (*diffusion*). Fresh blood must be supplied, in which the oxygen can be solved (*perfusion*). In oeMRI, oxygen acts as a weak contrast agent with an average oxygen-induced shortening of the T1 relaxation time of pulmonary parenchyma between 7 % and 14 % (4-14).

Several studies have shown that oeMRI is a feasible technique in healthy volunteers, but there is only limited experience in circumscribed patient cohorts such as patients suffering from PH (10, 11, 13, 15-21). The purpose of our study was two-fold. The first aim of this study was to assess the value of oeMRI in patients with PH, comparing oeMRI with V/Q scintigraphy serving as imaging reference standard. The second aim was to analyze oeMRI data with two different methods: The commonly used so-called "relative signal enhancement" (RSE) (4,11,14,15,22) and an improved "cross-correlation coefficient" (CCC) analysis, which allows for a faster post-processing by bypassing the process of selecting co-registered images (23, 24).

Materials and Methods

Subjects

Our study included 33 patients with PH (20 women; 13 men; 56.9±17.5 years; range 15 to 81 years). All patients underwent pulmonary V/Q scintigraphy and dynamic oeMRI within a period of 2 months (mean 10.5±14.3 days; range 1 to 59 days). According to all patient data available (i.e. clinical history, right cardiac catheterization, additional or previously conducted imaging like CT-angiography, scintigraphy or MRI) 25 of these 33 patients suffered from CTEPH, and 8 were diagnosed with IPAH. One patient had undergone pneumectomy due to a Schwannoma. Ethics committee approval was obtained, and all patients gave written informed consent before investigation.

V/Q scintigraphy

V/Q scintigraphy was performed in supine position and always in the following sequence: First, perfu-

sion images were acquired after intravenous administration of approximately 100 MBq technetium-99 m labeled macroaggregated albumin (99 mTc-MAA) during 3-5 respiratory cycles. We used an energy window of 20% (centered at the technetium-99m peak: 140 keV), a matrix of 128 × 128 pixels and accumulated approximately 400.000 counts per view. In a second step after a mean time delay of approximately 20 minutes, ventilation images were obtained after inhalation of graphite crucible microaerosol particles labelled with technetium-99 m pertechnetate (Technegas) delivered via a nebulizer. In order to ensure appropriate discrimination between the different information delivered by the perfusion and the ventilation images, a minimum threefold count rate (compared to the initial perfusion scan) was deemed necessary for the ventilation image acquisition. For all examinations, an ECAM dual-head Gamma-camera (Siemens Healthcare, Erlangen, Germany) with a medium-energy, general-purpose collimator was used. Anterior, posterior, lateral and oblique projections were obtained for both, the ventilation and the perfusion scans.

Oxygen-enhanced MRI of the lungs

All exams were performed on a whole-body MRI system with a field strength of 1.5 Tesla (Magnetom Sonata, Siemens Healthcare, Erlangen, Germany) with a gradient system providing a maximum gradient strength of 40 mT/m and a maximum gradient slope of 200 mT/(m ms). A dedicated parallel-imaging thorax surface coil system (Siemens Healthcare, Erlangen, Germany) consisting of 12 coil elements (6 posterior and 6 anterior) was used; 8 of these 12 elements are combined in pairs of 2 such that together with the remaining 4 elements the coil system matches the 8 receiver channels of the MR system.

We used a T1-weighted multi-slice inversion-recovery half-Fourier-acquisition single-shot turbo-spin-echo (HASTE) sequence (TI=1300 ms, TE=11 ms, 4 slices, slice thickness 8 mm, slice distance 16 mm, matrix 128×128, FOV 400×400 mm², GRAPPA acceleration factor 2).

It is known that altered physiology during breath holding occurs (25). In addition, many patients with PH are not able to hold their breath long enough for data acquisition, so we implemented a respiratory-triggered free-breathing acquisition technique and a cardiac triggering technique to decrease the motion artifacts, as described elsewhere (24-26). Images were acquired when diastole and end-expiration fitted together.

Each examination consisted of a series of 80 acquisitions (20×air, 20×O_2, 20×air, 20×O_2). The total acquisition time varied between 8 and 13 minutes depending on the respiration frequency, which was between 6/min and 10/min. Room air and oxygen from an air/oxygen providing connection in the examination room was supplied via an oxygen mask. The mask was fitted properly before the patients were examined in supine position. The gas flow was about 20 l/min.

Image post-processing and data analysis

V/Q scintigraphy data evaluation

V/Q scintigraphy data was rated by an experienced nuclear medicine physician blinded to the findings of oeMRI. Each lung was segmented in three areas (upper, middle, and lower area), resulting in six lung areas per patient. The acquired images were visually assessed for perfusion defects and ventilation defects in a dichotomous way (defect yes/no per lung area; 6 areas per patient).

oeMRI: motion correction and segmentation

As a first step of post-processing, a retrospective motion correction was performed as described in detail elsewhere (14). The vertical diaphragm position in all repetitions is compared with the diaphragm position in an average image, and only acquisitions with identical vertical diaphragm position within 3 pixels of cranio-caudal ranges are accepted for further processing. Then, the lungs were segmented manually in each acquired slice by defining two regions of interest (ROIs; right and left lung) excluding the large central pulmonary vessels.

oeMRI: relative-signal-enhancement analysis

For RSE calculation, the first 5 acquisitions after each switching of the gas supply were discarded because of their intermediate signal intensity. To reduce the influence of statistical noise, the image data were low-pass filtered before further processing using a 5×5 Gauss filter with a standard deviation of 2 pixels. Then, all accepted remaining images of room air measurements (mean navigator acceptance rate 75.8±17.0%) as well as of the oxy-

gen measurements (mean navigator acceptance rate 78.9±17.3%) were averaged, and maps of relative signal increase (SI) $\Delta SI_{rel} = (SI_{oxygen} - SI_{air})/SI_{air}$ were calculated.

oeMRI: cross-correlation coefficient analysis

The CCC analysis assesses the similarity between the temporal SI variations in time course data and a reference function and was applied without prior motion correction. In this study, the time response function of each pixel was correlated with a piecewise exponential function, which fits best with the physiologic signal increase due to oxygen inhalation (27); the exponential time constants for oxygen wash-in and wash-out were set to 30 s and 25 s, respectively. Deviating time constants, e. g., in diseased lung areas, will lead to reduced correlation coefficients. Following Molinari et al., pixels with a correlation coefficient of 0.5 or higher were counted as oxygen-activated pixels (OAP) (24).

oeMRI: qualitative and quantitative evaluation

Two blinded radiologists performed the visual, **qualitative** analysis of the reconstructed oeMRI images via consensus decision. For this evaluation, each lung was segmented in three areas as in the scintigraphy analysis **(Fig.1)**. If at least one defect was seen in a lung area in the reconstructed oeMRI images, this area was counted as "diseased". The visual analysis of the oeMRI images included assessment of both the RSE and CCC maps. The homogeneity of the signal was assessed in both maps as well (homogeneous or inhomogeneous).

If an examination was peculiar for an ultra low enhancement in all lung areas on all slices, it was unblinded and compared with the corresponding V/Q scintigraphy images. If an obvious discrepancy in terms of scale and severity occurred in this comparison, which was not explainable by disease related reasons (i.e. a real defect), the examination was considered not to be adequate for further diagnostic evaluation due to technical reasons.

For all diagnostically adequate examinations sensitivities and specificities of oeMRI in comparison to V/Q scintigraphy were calculated using a fourfold table.

Quantitative analysis of the oeMRI images included assessment of the mRSE, the mean cross-correlation coefficient (mCCC) and the fraction of oxygen-activated pixels (fOAP) in the selected ROIs (right and left lung). The correlation of all determined parameters with each other and with the number of diseased lung areas in the CCC maps and the RSE maps were statistically evaluated using the Spearman rank correlation coefficient test. SPSS (version 14.0; IBM company; Chicago; Illinois) was used for calculation.

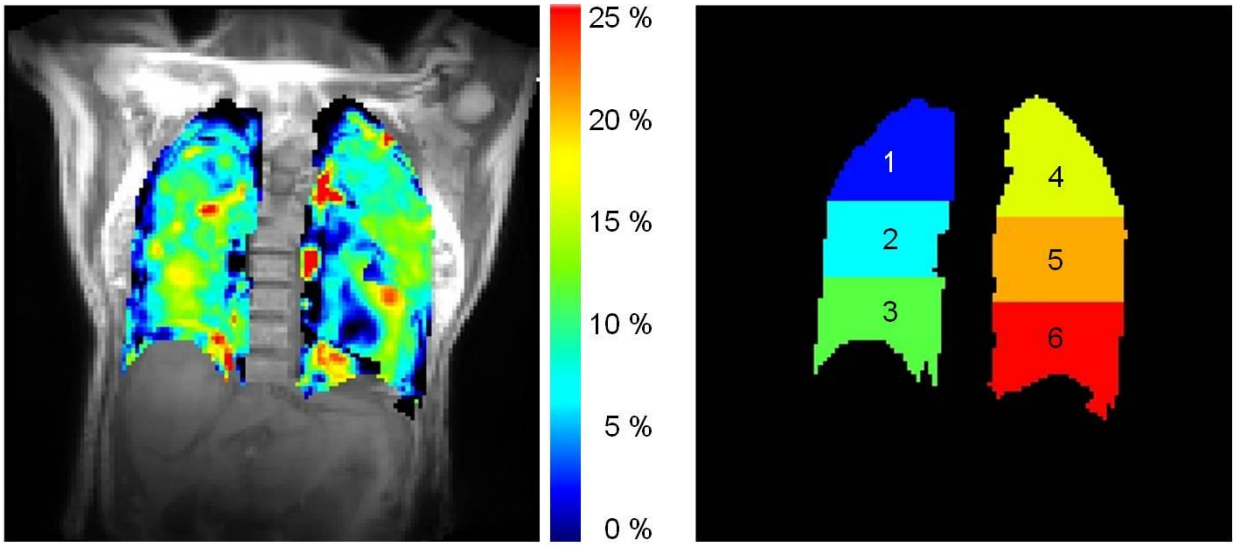

Figure 1: Example of an oeMRI examination (left) with segmented lungs (6 color-coded segmented fields, right). Both images show projections in anterior-posterior direction over all 4 acquired slices.

Results

oeMRI success rate and average oeMRI parameters

All dynamic oxygen-enhanced MR examinations were completed without any adverse effects such as headache, nausea, vomiting, dyspnea, or chest pain.

The average mRSE during oxygen breathing was 7.7±4.6% (range: 0.4% to 17.2%; values of n = 33 patients). The average mCCC was 0.42±0.17 (range 0.08 to 0.78; for n = 33 patients) and the mean fOAP was 40.0±28.6% (range 0.1% to 95.3%; values of n = 33 patients).

26 of the 33 examinations (79%) reached diagnostic image quality and were used for further evaluation. In this selected patient group, the average mRSE, mCCC and fOAP were 9.4±3.7%, 0.48±0.13, and 49.2±25.0%, respectively. The mean age of the included patients was 56.4±15.6 years in a range of 26 to 77 years. In the group of excluded patients (59.0±24.7 years; range 15 to 81 years) the corresponding mean mRSE, mCCC and fOAP were 1.5±0.9%, 0.20±0.08, and 6.1±7.6%, respectively. 6 of the included 26 patients suffered from IPAH and 20 from CTEPH. The aforementioned patient who underwent a pneumonectomy was included in this group. In one patient with an occlusion of the left main pulmonary artery, a thrombectomy was performed between the scintigraphy and the oeMRI examination; thus, only the untreated right lung was available for assessment. In total, 150 (=24×6 + 2×3) lung areas were available for evaluation.

V/Q scintigraphy

In the 26 patients (150 lung areas) who were available for analysis, ventilation scintigraphy showed 37 (25%) diseased and 113 (75%) healthy lung areas. The perfusion scintigraphy showed 96 (64%) diseased and 54 (36%) healthy areas.

oeMRI and V/Q scintigraphy: qualitative results and diagnostic accuracy

Applying the common form of post-processing, i. e., the RSE method, the sensitivity and specificity of the qualitative, subjective analysis of the oeMRI data compared to ventilation scintigraphy was 92% and 73%, for the detection of areas with decreased ventilation (defect yes/no). The comparison of the RSE maps with perfusion scintigraphy showed a sensitivity of 60% and a specificity of 87%. (**Table 1A,B**; **Figs. 2, 3**)

When applying the new approach for post-processing, i.e. the CCC method, for the qualitative analysis, sensitivity and specificity of oeMRI compared to ventilation scintigraphy were 89% and 81%. The comparison of the CCC maps with the perfusion scintigraphy lead to a sensitivity of 50% and a specificity of 87%. **(Table 1C,D**; **Figs. 2, 3**)

Table 1: Comparison of oeMRI vs. V/Q scintigraphy

	1A: oeMRI (RSE method) vs. ventilation scintigraphy			**1B: oeMRI (RSE method) vs. perfusion scintigraphy**		
	V scintigraphy positive	V scintigraphy negative	Σ	Q scintigraphy positive	Q scintigraphy negative	Σ
oeMRI (RSE method) positive	34	31	65 *(PPV 52%)*[3]	58	7	65 *(PPV 89%)*[3]
oeMRI (RSE method) negative	3	82	85 *(NPV 96%)*[4]	38	47	85 *(NPV 55%)*[4]
Σ	37 *(Sens. 92%)*[1]	113 *(Spec. 73%)*[2]	150 *(DA 77%)*[5]	96 *(Sens. 60%)*[1]	54 *(Spec. 87%)*[2]	150 *(DA 70%)*[5]

	1C: oeMRI (CCC method) vs. ventilation scintigraphy			**1D: oeMRI (CCC method) vs. perfusion scintigraphy**		
	V scintigraphy positive	V scintigraphy negative	Σ	Q scintigraphy positive	Q scintigraphy negative	Σ
oeMRI (CCC method) positive	33	22	55 *(PPV 60%)*[3]	48	7	55 *(PPV 87%)*[3]
oeMRI (CCC method) negative	4	91	95 *(NPV 96%)*[4]	48	47	95 *(NPV 49%)*[4]
Σ	37 *(Sens. 89%)*[1]	113 *(Spec. 81%)*[2]	150 *(DA 83%)*[5]	96 *(Sens. 50%)*[1]	54 *(Spec. 87%)*[2]	150 *(DA 63%)*[5]

[1] sensitivity, [2] specificity, [3] positive predictive value, [4] negative predictive value, [5] diagnostic accuracy

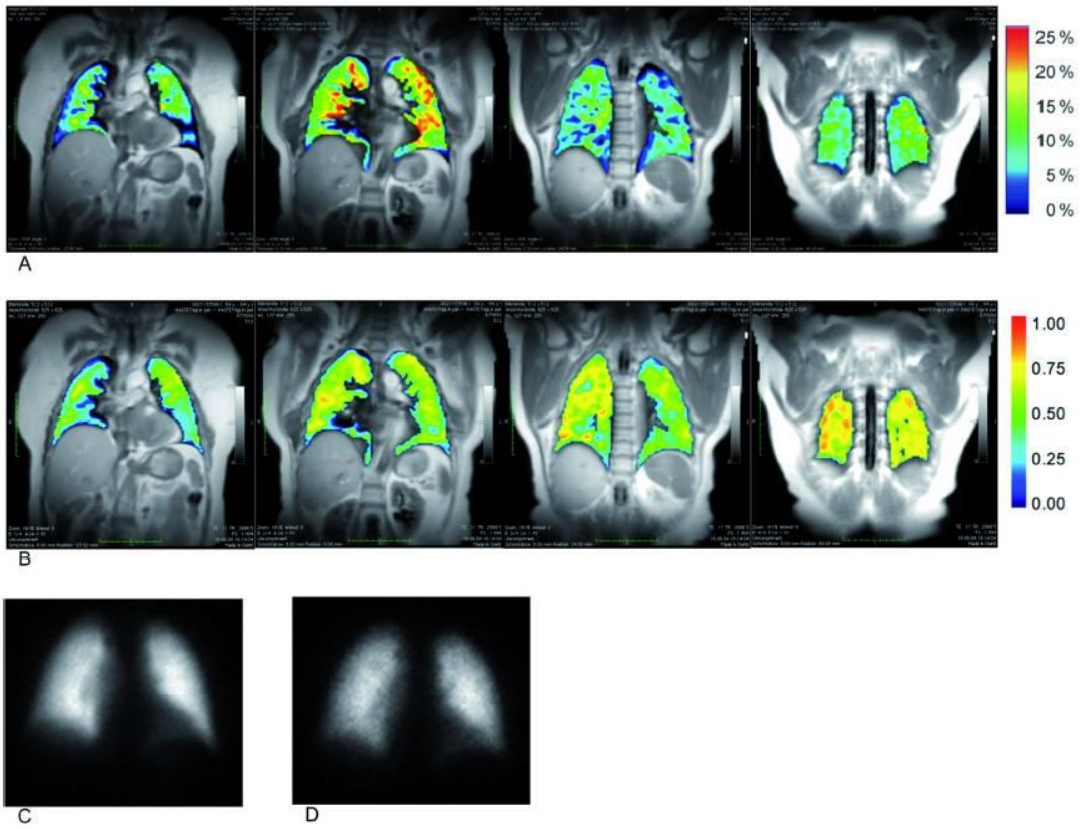

Figure 2: 64-year-old female patient without circumscribed defects. A: RSE maps with relatively homogenous SI after oxygen inhalation. B: CCC maps without defects and with an overall more homogeneous SI if compared with the RSE maps. C: Ventilation scintigraphy with regular ventilation. D: Perfusion scintigraphy without detectable perfusion defects.

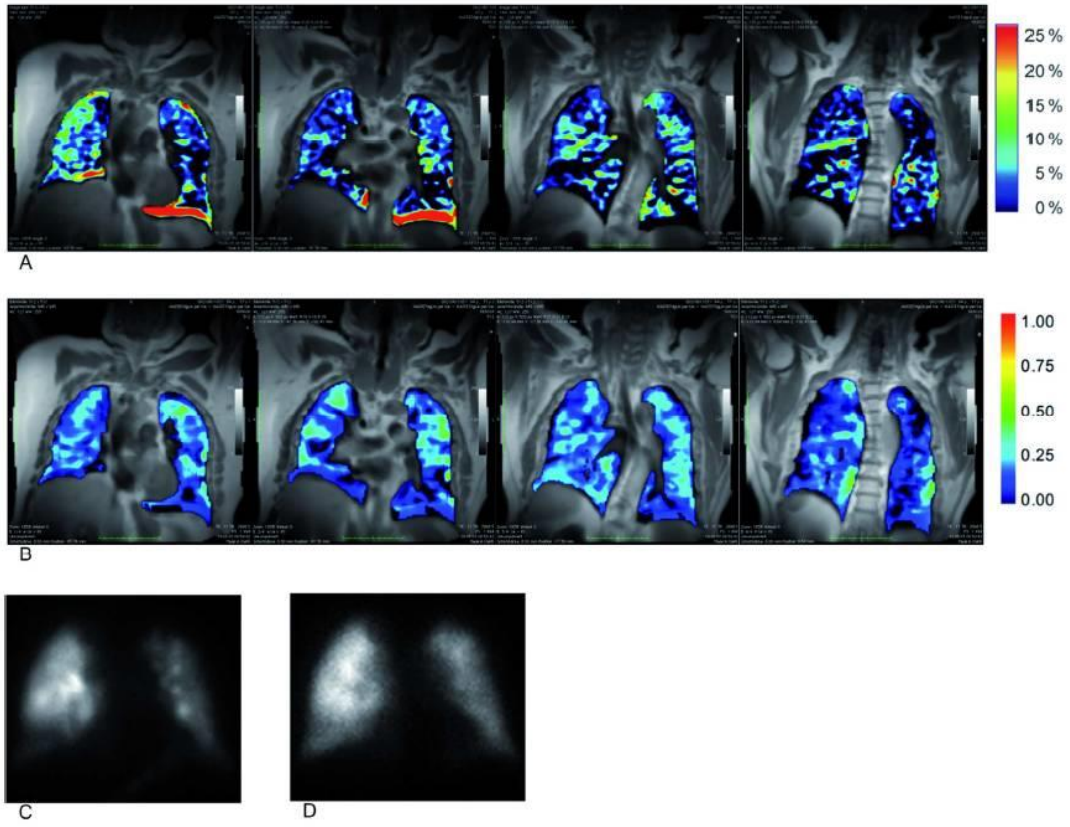

Figure 3: 78-year-old male patient. A: RSE maps with an overall lower SI in the left lung and an inhomogeneous enhancement accentuated in the lower right lung. B: CCC maps with relatively similar impression compared to the RSE maps. C: Ventilation scintigraphy with lowered ventilation in the left lung and in the lower right lung. D: Perfusion scintigraphy with perfusion defects similar to the ventilation scintigraphy.

oeMRI and V/Q scintigraphy: quantitative results

Analyzing only the correlations of the different oeMRI results, the quantitative analysis showed that the number of seen diseased lung areas in oeMRI RSE maps and CCC maps correlated significantly ($p < 0.001$, $r = 0.81$) as well as all combinations of the measured quantitative parameters fOAP, mCCC, and mRSE ($p < 0.01$). The fOAP and the mCCC showed a significant correlation with the number of diseased lung areas seen in oeMRI post-processed with the CCC method (fOAP correlation: $p = 0.006$, $r = 0.49$; mCCC correlation: $p = 0.003$, $r = 0.53$). Likewise, the mRSE and the number of diseased lung areas seen in the RSE maps correlated significantly ($p = 0.019$, $r = 0.41$). (**Table 2**)

Comparing oeMRI and V/Q scintigraphy, the quantitative analysis showed that the number of seen diseased lung areas in oeMRI RSE maps and CCC maps correlated significantly with the number of seen diseased lung areas in the ventilation and perfusion scintigraphy
(RSE maps vs. V scintigraphy: $p = 0.001$, $r = 0.58$; RSE maps vs. Q scintigraphy: $p = 0.001$, $r = 0.57$; CCC maps vs. V scintigraphy: $p < 0.001$, $r = 0.73$; CCC maps vs. Q scintigraphy: $p = 0.017$, $r = 0.42$). Furthermore, mRSE showed a significant correlation with the number of seen diseased lung areas in the ventilation scintigraphy ($p = 0.032$, $r = 0.37$), but failed to reach the significance level in the correlation with the perfusion scintigraphy (as well as all other combinations of the evaluated parameters). (**Table 2**)

Table 2: Correlation of mRSE, mCCC and fOAP with each other and with the number of diseased lung areas in oeMRI and scintigraphy

			Spearman's rho	p-value
mRSE	vs.	RSE maps[1]	0.41	0.019*
	vs.	CCC maps[2]	0.43	0.014*
	vs.	V scintigraphy[3]	0.37	0.032*
	vs.	Q scintigraphy[4]	0.06	0.39
	vs.	mCCC	0.56	0.001*
	vs.	fOAP	0.55	0.002*
mCCC	vs.	RSE maps[1]	0.35	0.042*
	vs.	CCC maps[2]	0.53	0.003*
	vs.	V scintigraphy[3]	0.28	0.08
	vs.	Q scintigraphy[4]	0.03	0.44
	vs.	fOAP	0.97	< 0.001*
fOAP	vs.	RSE maps[1]	0.30	0.071
	vs.	CCC maps[2]	0.49	0.006*
	vs.	V scintigraphy[3]	0.27	0.095
	vs.	Q scintigraphy[4]	0.06	0.39

[1] number of diseased lung areas in oeMRI post-processed with the RSE method
[2] number of diseased lung areas in peMRI post-processed with the CCC method
[3] number of diseased lung areas in ventilation scintigraphy
[4] number of diseased areas in perfusion scintigraphy
* statistically significant

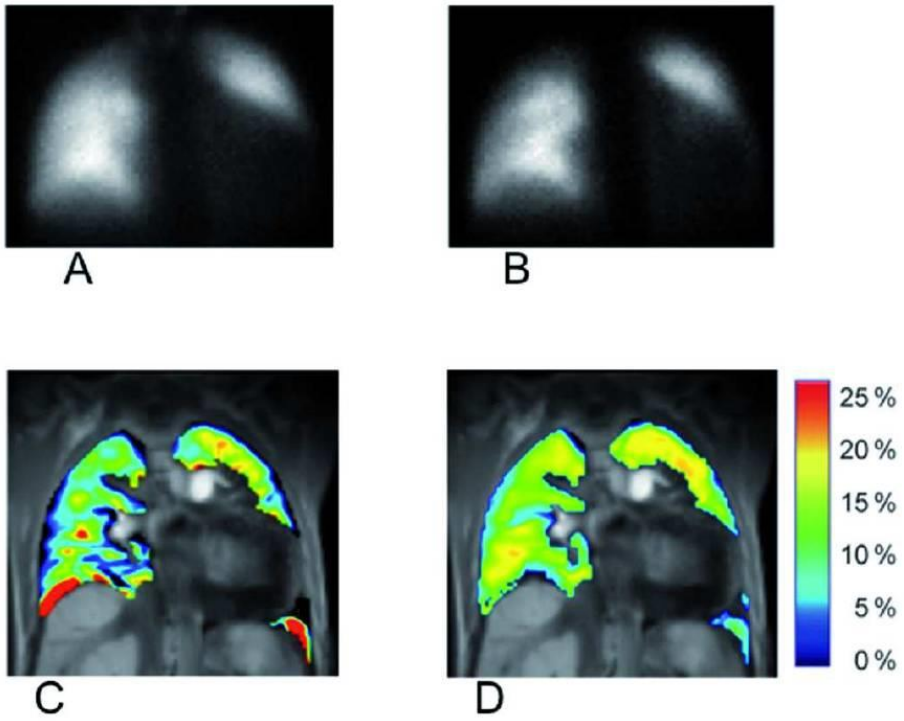

Figure 4: 46-year-old female patient with lowered SI in the left lung dependent on either an enlarged heart or a combined ventilation perfusion defect. A: Ventilation scintigraphy with lowered signal in the left lower lung. B: Perfusion scintigraphy with lowered signal in the left lower lung. C: With the morphologic information of the RSE map, the observed lower signal is identified as an enlarged heart. D: The morphologic information of the CCC map also allows the identification of the enlarged heart.

Discussion

Pulmonary hypertension is a severe disease with various underlying causes. Therefore, imaging is an important tool for the primary diagnosis and for monitoring the course of the disease. Common imaging methods applied in PH-patients, such as V/Q scintigraphy and CT, are disadvantaged by the use of ionizing radiation. This is an important limitation, especially if follow-up examinations in younger patients suffering from PH are necessary. oeMRI is an interesting alternative imaging method which does not apply ionizing radiation and can therefore be used for repeated follow-up examinations. In addition, oeMRI provides superior morphological information compared to scintigraphy, as in scintigraphy it may sometimes be difficult to clearly distinguish an enlarged heart from a combined ventilation/perfusion defect (see **Fig. 4**). Thus, the aim of the present study was to test the potential clinical value of oeMRI in a selected patient cohort suffering from PH.

The diagnostic accuracy of oeMRI was evaluated to decide whether or not oeMRI may become a useful tool in assessing PH and whether the more robust CCC method can substitute the conventional RSE post-processing method. For this qualitative assessment, we compared oeMRI with V/Q scintigraphy (see **Figs. 2** and **3**) and found high sensitivity and specificity rates between oeMRI (independent of the post-processing method) and ventilation scintigraphy. It has been stated that oeMRI not only shows ventilation, but a combination of diffusion and ventilation (8, 15). The observed, higher correlation of oeMRI and ventilation scintigraphy compared to the lower correlation with perfusion scintigraphy is in agreement with earlier studies, which demonstrated a preserved oeMRI signal in the presence of perfusion defects (4, 28). One possible explanation may be that even lung areas with reduced blood flow – observed as perfusion defects in perfusion scintigraphy – still contain a sufficiently high blood volume, in which the inhaled oxygen can be dissolved, resulting in a signal increase of this lung area.

These results are also reflected in our comparison of the numbers of diseased lung areas between the different modalities (oeMRI an V/Q Scintigraphy). Spearman's rank correlation coefficient showed quite variable results, with only moderate correlation of CCC maps vs. Q scintigraphy ($r =$

0.42), but a good correlation of CCC maps vs. V scintigraphy ($r = 0.73$).

In addition to visual changes, oeMRI provides quantitative parameters to assess the severity of a disease, such as the mean relative signal enhancement. The mRSE correlated significantly with the number of diseased lung areas in both ventilation scintigraphy and in oeMRI maps (either post-processed with the RSE or CCC method). Another interesting quantitative parameter is the fraction of oxygen-activated pixels (with a cross-correlation coefficient of 0.5 or higher) (24, 27), which can be considered as an indicator for the amount of healthy lung tissue. The fOAP (respectively the fraction of *non*-activated pixels; 100 % – fOAP) showed a high correlation with the number of diseased areas seen in oeMRI post-processed with the CCC method. The statistically significant results, however, are only associated with moderate (e.g. mRSE vs. mCCC $r = 0.56$) or low (e.g. mRSE vs. number of diseased lung areas in V scintigraphy $r = 0.37$) correlation coefficients. Nevertheless, our results suggest that quantitative oeMRI parameters such as the mRSE or fOAP could be serving as markers for the severity of PH, even if their predictive value is somewhat limited.

The applied respiratory-triggered multislice oeMRI protocol results in average acquisition times between 8 and 13 min for a complete multislice data set (with 4 to 6 slices), depending on the patients' respiration frequency and heart rate (14). This relatively short acquisition time (as compared to e.g., 6 minutes/slice without respiratory triggering in earlier approaches (29)) offers the possibility to implement oeMRI in a clinical routine setting in combination with other MRI examinations, such as morphologic MRI of the lung, pulmonary high-resolution MR angiography and contrast-enhanced perfusion MRI, or right-heart cardiac MRI. This combination of ventilation/diffusion-sensitive oeMRI with other techniques enables a further differentiation of the underlying cause of an observed oeMRI-defect (16, 26).

In our study we observed a dropout rate of 21 % of all oeMRI datasets due to a non-diagnostic image quality, which agrees well with the dropout rate reported by Nakagawa et al. (16). Patients were only excluded, if two requirements were fulfilled: First, the enhancement after oxygen inhalation in all lung areas in all slices had to be extremely low (i.e. hardly any signal in the qualitative visual assessment). Second, after unblinding the reference imaging data of the V/Q scans, there had to be an obvious discrepancy between the defects in the corresponding V/Q scintigraphy and the oeMRI images. The simultaneous occurrence of these two requirements indicates that the decreased oxygen enhancement is not disease-related, but rather caused by technical issues (e.g., an untight breathing mask) or a patient failure (i.e., low depth of inspiration in general). However, the examination was considered to be diagnostically adequate despite its overall low enhancement, if only one lung area in one slice had shown an almost normal enhancement or if the defects in the comparing V/Q scintigraphy matched the oeMRI images in terms of scale and severity after unblinding. It is difficult to decide whether this dropout rate is associated with pulse sequence limitations, with the gas supply or oxygen mask, with the individually different response of different patients to the supplied oxygen, or with a low depth of inspiration. Modifications of the acquisition technique such as alteration of the ECG and/or respiratory triggering might be a way to further decrease the dropout rate. In addition, it is necessary to advise the patients properly of how to breathe correctly and sufficiently for this kind of examination.

The post-processing of oeMRI data used in the present study (including motion correction and cross-correlation analysis) is technically challenging, and there is no commercially available post-processing tool for oeMRI at present. However, post-processing with the proposed CCC method spares the step of discarding motion-impaired images and therefore represents a rather quick and simple analysis of the complex oeMRI data. To assess the value of oeMRI with the CCC method in particular, we chose the number of observed diseased areas as a quantitative parameter for diagnostic comparability. The high correlation between the number of seen diseased areas in RSE-based oeMRI maps and in CCC-based oeMRI maps indicates that there is no substantial difference between these two methods in terms of visual image assessment, and that CCC provides a comparable diagnostic accuracy as the standard RSE method. Moreover, both post-processing techniques provid-

ed a significant correlation between the number of seen diseased lung areas in oeMRI and the number of seen diseased lung areas observed in ventilation and perfusion scintigraphy. Taking the observed sensitivities and specificities into account, this indicates a moderate diagnostic comparability between oeMRI and V/Q scans, with a good sensitivity of oeMRI as compared especially with ventilation scintigraphy.

However, the specificities and sensitivities varied a bit depending on the post-processing method applied. This point is reflected in the results, where the CCC method was superior in its specificity but inferior in its sensitivity as compared to results of the RSE method when compared to V/Q scintigraphy. This is probably due to the fact that there is limited experience with the visual interpretation of the parameter maps, especially assessing data post-processed with the CCC method. The visual assessment may also be additionally influenced by the fact that images post-processed with the CCC method seemed to have a more homogenous visual aspect when compared to RSE images (see **Fig. 2**).

Further refinements in the post-processing will potentially provide additional information about the lung function, e.g., wash-in and wash-out time courses of oxygen in dynamic examinations. There are some studies suggesting that these additional dynamic parameters may be useful in evaluating the lung function in PH patients (12, 20, 30, 31).

Limitations of the present study include an only moderate sample size (n=26 evaluated patients); in a disease with various underlying causes such as PH it might be necessary to assess a larger patient cohort, to substantiate our results. Furthermore, our approach of oeMRI is based exclusively on relative signal changes, which depend on several parameters such as the underlying intrinsic T1 relaxation time of lung tissue and the inversion time. Under certain circumstances, reduced local oxygen concentration due to ventilation defects might even be compensated by disease-related changes in intrinsic T1, thus potentially concealing ventilation changes in a lung area. An approach to overcome this effect is to quantify the T1 relaxation time in separate T1 measurements at room air and oxygen inhalation (12, 13) however, these time-consuming additional acquisitions were beyond the scope of our study.

In conclusion, oeMRI has been demonstrated to be feasible in PH-patients, yielding a relatively high agreement in terms of sensitivity and specificity with ventilation scintigraphy, but a somewhat limited sensitivity compared to perfusion scintigraphy. In addition, our study showed that post-processing with an improved fast cross-correlation method is reliable, and that quantitative parameters provided by oeMRI, such as the mean relative signal enhancement, may be additional helpful tools in assessing the severity of PH or of other lung diseases.

References

1. Galie N, Hoeper MM, Humbert M, et al. Guidelines for the diagnosis and treatment of pulmonary hypertension: The Task Force for the Diagnosis and Treatment of Pulmonary Hypertension of the European Society of Cardiology (ESC) and the European Respiratory Society (ERS), endorsed by the International Society of Heart and Lung Transplantation (ISHLT). Eur Heart J 2009;30(20):2493-2537.
2. Park MH. Advances in diagnosis and treatment in patients with pulmonary arterial hypertension. Catheter Cardiovasc Interv 2008;71(2):205-213.
3. Fedullo PF, Auger WR, Kerr KM, Rubin LJ. Chronic thromboembolic pulmonary hypertension. N Engl J Med 2001;345(20):1465-1472.
4. Edelman RR, Hatabu H, Tadamura E, Li W, Prasad PV. Noninvasive assessment of regional ventilation in the human lung using oxygen-enhanced magnetic resonance imaging. Nat Med 1996;2(11):1236-1239.
5. Kauczor HU, Kreitner KF. MRI of the pulmonary parenchyma. Eur Radiol 1999;9(9):1755-1764.
6. Stock KW, Chen Q, Morrin M, Hatabu H, Edelman RR. Oxygen-enhanced magnetic resonance ventilation imaging of the human lung at 0.2 and 1.5 T. J Magn Reson Imaging 1999;9(6):838-841.
7. Kauczor HU, Kreitner KF. Contrast-enhanced MRI of the lung. Eur J Radiol 2000;34(3):196-207.
8. Loffler R, Muller CJ, Peller M, et al. Optimization and evaluation of the signal intensity change in multisection oxygen-enhanced MR lung imaging. Magn Reson Med 2000;43(6):860-866.
9. Muller CJ, Loffler R, Deimling M, Peller M, Reiser M. MR lung imaging at 0.2 T with T1-weighted true FISP: native and oxygen-enhanced. J Magn Reson Imaging 2001;14(2):164-168.
10. Ohno Y, Chen Q, Hatabu H. Oxygen-enhanced magnetic resonance ventilation imaging of lung. Eur J Radiol 2001;37(3):164-171.
11. Ohno Y, Hatabu H, Takenaka D, Van Cauteren M, Fujii M, Sugimura K. Dynamic oxygen-enhanced MRI reflects diffusing capacity of the lung. Magn Reson Med 2002;47(6):1139-1144.

12. Arnold JF, Fidler F, Wang T, Pracht ED, Schmidt M, Jakob PM. Imaging lung function using rapid dynamic acquisition of T1-maps during oxygen enhancement. MAGMA 2004;16(5):246-253.
13. Jakob PM, Wang T, Schultz G, Hebestreit H, Hebestreit A, Hahn D. Assessment of human pulmonary function using oxygen-enhanced T(1) imaging in patients with cystic fibrosis. Magn Reson Med 2004;51(5):1009-1016.
14. Dietrich O, Losert C, Attenberger U, et al. Fast oxygen-enhanced multislice imaging of the lung using parallel acquisition techniques. Magn Reson Med 2005;53(6):1317-1325.
15. Muller CJ, Schwaiblmair M, Scheidler J, et al. Pulmonary diffusing capacity: assessment with oxygen-enhanced lung MR imaging preliminary findings. Radiology 2002;222(2):499-506.
16. Nakagawa T, Sakuma H, Murashima S, Ishida N, Matsumura K, Takeda K. Pulmonary ventilation-perfusion MR imaging in clinical patients. J Magn Reson Imaging 2001;14(4):419-424.
17. Ohno Y, Hatabu H, Higashino T, et al. Oxygen-enhanced MR imaging: correlation with postsurgical lung function in patients with lung cancer. Radiology 2005;236(2):704-711.
18. Ohno Y, Hatabu H, Takenaka D, Adachi S, Van Cauteren M, Sugimura K. Oxygen-enhanced MR ventilation imaging of the lung: preliminary clinical experience in 25 subjects. AJR Am J Roentgenol 2001;177(1):185-194.
19. Ohno Y, Iwasawa T, Seo JB, et al. Oxygen-enhanced magnetic resonance imaging versus computed tomography: multicenter study for clinical stage classification of smoking-related chronic obstructive pulmonary disease. Am J Respir Crit Care Med 2008;177(10):1095-1102.
20. Ohno Y, Koyama H, Nogami M, et al. Dynamic oxygen-enhanced MRI versus quantitative CT: pulmonary functional loss assessment and clinical stage classification of smoking-related COPD. AJR Am J Roentgenol 2008;190(2):W93-99.
21. Stadler A, Stiebellehner L, Jakob PM, et al. Quantitative and o(2) enhanced MRI of the pathologic lung: findings in emphysema, fibrosis, and cystic fibrosis. Int J Biomed Imaging 2007;2007:23624.
22. Arnold JF, Kotas M, Fidler F, Pracht ED, Flentje M, Jakob PM. Quantitative regional oxygen transfer imaging of the human lung. J Magn Reson Imaging 2007;26(3):637-645.
23. Mai VM, Tutton S, Prasad PV, et al. Computing oxygen-enhanced ventilation maps using correlation analysis. Magn Reson Med 2003;49(3):591-594.
24. Molinari F, Eichinger M, Risse F, et al. Navigator-triggered oxygen-enhanced MRI with simultaneous cardiac and respiratory synchronization for the assessment of interstitial lung disease. J Magn Reson Imaging 2007;26(6):1523-1529.
25. Ley S, Puderbach M, Risse F, et al. Impact of oxygen inhalation on the pulmonary circulation: assessment by magnetic resonance (MR)-perfusion and MR-flow measurements. Invest Radiol 2007;42(5):283-290.
26. Ohno Y, Hatabu H. Basics concepts and clinical applications of oxygen-enhanced MR imaging. Eur J Radiol 2007;64(3):320-328.
27. Dietrich O, Attenberger UI, Ingrisch M, et al. Analysis of signal dynamics in oxygen-enhanced magnetic resonance imaging. Invest Radiol 2010;45(4):165-173.
28. Chen Q, Levin DL, Kim D, et al. Pulmonary disorders: ventilation-perfusion MR imaging with animal models. Radiology 1999;213(3):871-879.
29. Mai VM, Chen Q, Bankier AA, Edelman RR. Multiple inversion recovery MR subtraction imaging of human ventilation from inhalation of room air and pure oxygen. Magn Reson Med 2000;43(6):913-916.
30. Naish JH, Parker GJ, Beatty PC, et al. Improved quantitative dynamic regional oxygen-enhanced pulmonary imaging using image registration. Magn Reson Med 2005;54(2):464-469.
31. Hatabu H, Tadamura E, Chen Q, et al. Pulmonary ventilation: dynamic MRI with inhalation of molecular oxygen. Eur J Radiol 2001;37(3):172-178.